Cathodoluminescence study of the influence of misfit dislocations on hole accumulation in an *n*-AlGaAs/*p*-GaAs/*n*-InGaAs heterojunction phototransistor

H. T. Lin and D. H. Rich[a)]
Photonic Materials and Devices Laboratory, Department of Materials Science and Engineering, University of Southern California, Los Angeles, California 90089-0241

O. Sjölund, M. Ghisoni, and A. Larsson
Chalmers University of Technology, Department of Optoelectronics and Electrical Measurements, S-412 96 Göteborg, Sweden

(Received 8 April 1996; accepted for publication 28 June 1996)

We have studied the influence of misfit dislocations on hole accumulation in the base layer of an *n*-AlGaAs/*p*-GaAs/*n*-InGaAs heterojunction phototransistor (HPT). Spatially and temporally resolved cathodoluminescence (CL) measurements reveal that variations in the hole accumulation is caused primarily by strain-induced defects which impede the transport of holes in the collector. The lifetime of holes in the InGaAs/GaAs collector is found to be negligibly affected by the underlying misfit dislocations in the InGaAs/GaAs collector. The reduction in the local electron-beam-induced current signal by the dislocations is less than ~20%, indicating that these defects have a minor impact on the overall device performance. © *1996 American Institute of Physics.* [S0003-6951(96)00937-0]

Heterojunction phototransistors (HPTs) composed of AlGaAs/GaAs/InGaAs are of particular importance as they can be vertically integrated into dense arrays for applications in parallel optical signal processing.[1–3] Owing to the increasing maturity of III–V epitaxial growth techniques, the AlGaAs/GaAs/InGaAs system is a leading candidate for HPTs that require transparent substrates at its photosensitive wavelengths. Absorber layers of InGaAs/GaAs multiple quantum wells (MQWs) are used to provide the photosensitivity. Due to the lattice mismatch, an increase in InGaAs QW thickness beyond a critical thickness for the formation of misfit dislocations, in an attempt to enhance its photosensitivity, could suffer a defect-induced reduction in current gain as the trade off. The current gain of an *npn*-type HPT depends strongly on the hole accumulation in the base.[2–4] Hole accumulation is a two step process that involves (i) escape of holes out of the quantum wells and transport to the base followed by (ii) recombination at the base-emitter junction. It is the aim of this letter to explore the influence of misfit dislocations on local variations in hole accumulation and demonstrate the degree to which defects can impact the HPT performance. In order to accomplish this we use a unique combination of spatially, spectrally, and temporally resolved cathodoluminescence (CL) and electron beam-induced current (EBIC) measurements to probe the influence of defects on the efficiency of hole collection.

The AlGaAs/GaAs/InGaAs resonant cavity enhanced HPT structure studied here was grown by Epitaxial Products International who used low pressure metalorganic chemical vapor deposition.[3,4] The sample growth, on an n^+-GaAs substrate miscut 2° off (100), was initiated by an n^+-GaAs (3×10^{18} cm^{-3}) buffer layer, after which a high reflectivity n^+-AlAs/GaAs (3×10^{18} cm^{-3}) quarter-wave stack was grown. Next, a 3940 Å n^+-GaAs subcollector (3×10^{18} cm^{-3}) and a 4410 Å InGaAs/GaAs MQW collector (5×10^{16} cm^{-3}) were grown. The MQW structure is composed of three groups of three 80 Å $In_{0.12}Ga_{0.88}As$ QWs that are separated by 360 Å GaAs barriers within each group and a center-to-center spacing of 1325 Å between groups. Finally, a 1000 Å *p*-GaAs (5×10^{17} cm^{-3}) base, a 1800 Å *n*-$Al_{0.3}Ga_{0.7}As$ emitter (5×10^{17} cm^{-3}), an 840 Å n^+-$Al_{0.3}Ga_{0.7}As$ layer (3×10^{18} cm^{-3}), and a 1400 Å n^+-GaAs (3×10^{18} cm^{-3}) contact layer were grown. A schematic of the band structure is shown in Fig. 1. For *in vacuo* biasing experiments, a AuGe/Ni/Au alloy was deposited on the sample surface to form an Ohmic contact with the n^+ GaAs contact layer, and subsequently Au wire bonded for external control of the applied voltage, V_{dc}, between the emitter and grounded collector. The HPT's photoresponse and current–voltage characteristics have been previously reported.[3,4]

The CL experiments were performed with a modified

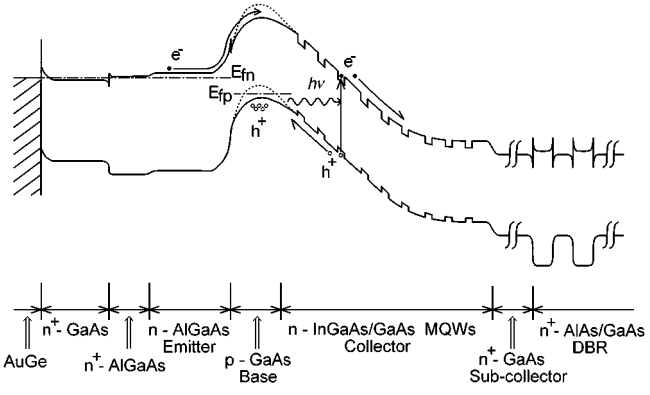

FIG. 1. Energy band structure of an AlGaAs/GaAs/InGaAs RCE-HPT device in an open-base, common collector configuration with an applied bias across the emitter collector.

a)Author to whom correspondence should be addressed. Electronic mail: danrich@alnitak.usc.edu

 0003-6951/96/69(11)/1602/3/$10.00

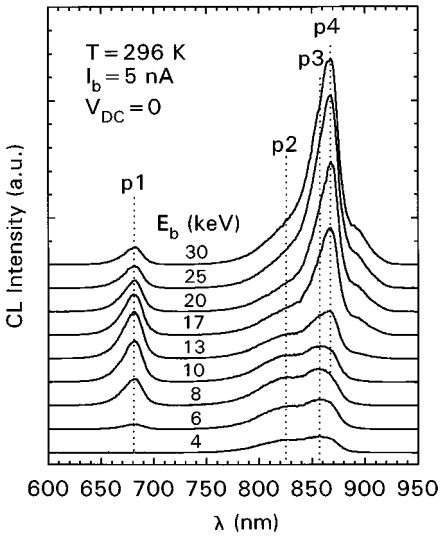

FIG. 2. Constant excitation CL spectra taken with various electron beam energies in the $4 \leqslant E_b \leqslant 30$ keV range at room temperature.

JEOL-840A scanning electron microscope (SEM) with electron beam energy, E_b, varying from 4 to 30 keV and with a probe current, I_b, of 5 nA. Time-resolved CL experiments were performed with the method of delayed coincidence in an inverted single photon counting mode, with a time resolution of ~100 ps.[5] Electron beam pulses of 50 ns width with a 1 MHz repetition rate were used to excite the sample. The luminescence signal was dispersed by a 1/4 m monochromator and detected by either a cooled GaAs:Cs PMT (for $\lambda \lesssim 900$ nm) or a Ge p-i-n detector ($\lambda \gtrsim 900$ nm).

Results of CL spectroscopy with various E_b at room temperature are shown in Fig. 2. The high energy peak (labeled $p1$) at $\lambda = 681$ nm represents the near-band-edge emission feature in $Al_{0.3}Ga_{0.7}As$ layers. As E_b increases, the $p1$ peak increases monotonically for $E_b \leqslant 13$ keV and then decreases when $E_b \geqslant 13$ keV. The beam energy of 13 keV corresponds to the position of the maximum electron-hole pair creation at ~0.3 μm beneath the surface,[6] which is consistent with the position of the AlGaAs–GaAs (emitter-base) interface. When E_b is as low as 4 keV, less than that necessary for detectable $p1$ emission, lower energy peaks at $\lambda = 825$ and $\lambda = 858$ nm (labeled $p2$ and $p3$, respectively) are observed. Thus, $p2$ and $p3$ originate from emission in the near-surface layers. These peaks are attributed to spatially indirect free exciton (e-h) transitions near the n^+-$Al_{0.3}Ga_{0.7}As/n^+$-GaAs interface. For $E_b \geqslant 13$ keV, a rapid rise in $p4$ ($\lambda = 868$ nm), corresponding to the GaAs near-band edge emission at room temperature, is observed. The rise in $p4$ is attributed to emission originating from GaAs layers lying deeper than the AlGaAs layers ($p1-p3$). CL depth-profiling measurements were also performed at $T = 87$ K. An additional emission centered at ~915 nm due to $e1-hh1$ transitions in the $In_{0.12}Ga_{0.88}As$/GaAs MQW is denoted by $p5$. The resulting CL intensities of $p1-p5$ vs E_b are shown in Fig. 3. The shift of the $p5$ curve towards larger E_b relative to peaks $p1-p4$ shows that $p4$ emission originates from the p-type GaAs base while $p5$ is due to emission from the MQW.

Monochromatic CL images ($E_b = 20$ keV, $I_b = 5$ nA,

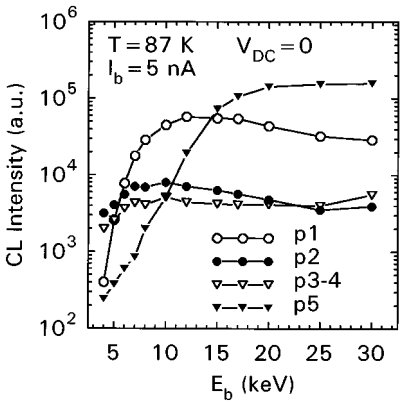

FIG. 3. CL intensities for different peaks $p1-p5$ as a function of electron beam energy E_b at $T = 87$ K.

$T = 295$ K, and $V_{dc} = -1$ V) were taken of the same region at $\lambda = 868$, 965, and 681 nm, as shown in Figs. 4(a)–4(c). A one-to-one spatial correlation of dark line defects (DLDs) is found in Figs. 4(a) and 4(b) (corresponding to $p4$ and $p5$ emission, respectively) but absent in Fig. 4(c) ($p1$ emission). The reduction of $p5$ at the DLDs is attributed to nonradiative recombination near misfit dislocations or point defects in the $In_{0.12}Ga_{0.88}As$/GaAs MQW.[4] The simultaneous reduction of $p4$ emission at DLDs indicates that these same defects reduce the accumulation of holes in the base. The luminescence efficiency of the base region decreases with a reduction in the accumulation of holes, owing to a reduced carrier recombination. This is further corroborated by the $\langle 110 \rangle$ line scan analysis shown in Fig. 5, where line scans are shown with arbitrary vertical offsets on a log scale. The dips in the CL intensity represent the reduction in the $p4$ emission which shows a ~20% reduction for $V_{dc} \geqslant 0$ in Fig. 5(a). For $V_{dc} < 0$, there are two important changes. First, there is a reduction in the total $p4$ ($\lambda = 868$ nm) CL intensity by ~50% as V_{dc} is reduced from 0 to -4 V. Second, the relative variation in the $p4$ emission reduces from ~20% to ~12% over the $0 \leqslant V_{dc} \leqslant -4$ V range. As the bias becomes more negative, the base-collector junction experiences an increasing reverse bias and the depletion region expands mainly into the MQW collector region due to the higher doping density in the base. For the negative bias in the first result above, the electrons generated near the base will experience an enhanced field-induced drift towards the collector, thereby reducing the number of electrons (minority carriers) which recombine radiatively in the base and resulting in a decreased $p4$ emission intensity. In the second result, the increased

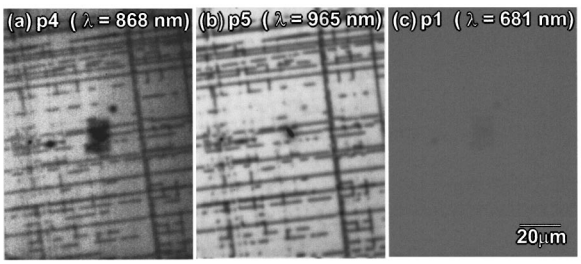

FIG. 4. Monochromatic CL images for $p4$ (a), $p5$ (b), and $p1$ (c) at room temperature.

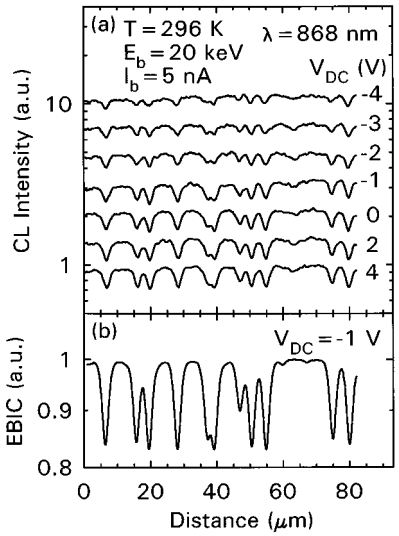

FIG. 5. Line scans of the $p4$ CL intensity (a) at various bias in $-4 \leqslant V_{dc} \leqslant 4$ eV range, and an EBIC line scan (b) over the same region at room temperature.

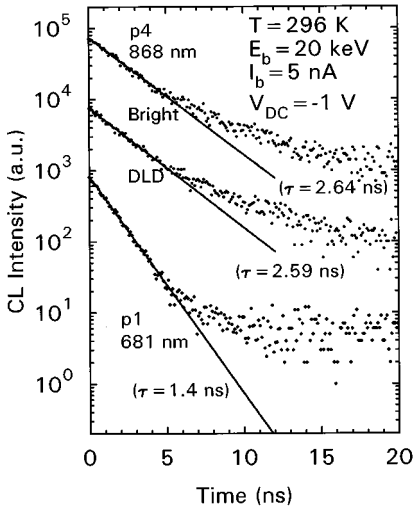

FIG. 6. CL decay transients for $p1$ and $p4$ in both a dark and a bright region (i.e., away from the DLD) at room temperature. Linear fits to the initial CL decay in the log scale are shown.

field in the MQW collector will enhance the efficiency of hole collection in the base. It is evident that the increased field will also reduce the relative impact of defect-generated potential fluctuations in the MQW on the drift of holes in the collector towards the base, resulting in the measured decrease in the $p4$ CL intensity variations caused by the DLDs. There is, however, no measurable change in the relative spatial variation in the $p5$ CL intensity when the bias is varied over the same $-4 \leqslant V_{dc} \leqslant 4$ V range. These results are direct evidence that the misfit dislocations in the collector region affect the accumulation of holes in the base by primarily impeding the carrier transport.

Hole accumulation in the base will also be affected by the minority carrier lifetime in the base. We performed time-resolved CL measurement at regions in varying proximity to the DLDs to search for spatial variations in the luminescence decay time. The CL transients for the decay of the $p4$ and $p1$ emissions taken near dark and bright regions (near and away from DLDs as in Fig. 4) are shown in Fig. 6. The initial luminescence decay time of $p1$, as measured from the slope in the semilog plot of CL intensity versus time, is 1.40 ns. For $p1$, this was found to be independent of the spatial position near DLDs, as expected from the homogeneous CL image of Fig. 4(c). The initial luminescence decay time of $p4$ for bright and dark regions are 2.64 and 2.59 ns, respectively. Several other bright and dark regions not shown also exhibit this luminescence decay time, independent of position within the overall time resolution of $\sim$100 ps. The apparent constancy of the decay time for the $p4$ peak shows that holes reaching the base are not directly affected by the underlying misfit dislocations in the MQW collector region. If misfit dislocation were to directly influence the $e-h$ recombination in the base, we would expect a spatial variation in the luminescence decay time correlated with the DLD position. The EBIC line scan in Fig. 5(b) reveals that defects giving rise to DLDs also reduce locally the collection of holes in the base and the field-induced drift of electrons towards the collector by $\sim$20%. For a spatially averaged EBIC or photocurrent measurement, the expected defect-induced reduction of the collector current is therefore $\sim$20% for a linear dislocation density of 10^4 cm^{-1}, or 1 dislocation per μm since the minority carrier diffusion length is ~ 1 μm. For the present sample, an estimated average linear dislocation density of $\sim 1.5 \times 10^3$ cm^{-1} (as observed in Fig. 4) scales into a 3% defect-induced reduction of the collector current. Therefore, for related HPT structures in general, when the dislocation density is kept sufficiently small($\sim 10^3$ cm^{-1}) and below the density at which dislocation pileups occur, an optimum device performance can be expected.

In conclusion, a variety of spatially, spectrally, and temporally resolved CL results shows that the spatial variation in the hole accumulation in an AlGaAs/GaAs/InGaAs HPT is caused primarily by strain-induced defects which impede the transport of holes to the base. The lifetime of collected holes in the base is found to be negligibly affected by the underlying misfit dislocations in the InGaAs/GaAs collector. Complementary EBIC measurements reveal that the defects have a relatively small impact on overall device performance provided the defect density is kept sufficiently small in the photosensitive collector.

This work was supported by ARO and NSF (RIA-ECS) and was also sponsored by the Swedish Research Council for Engineering Sciences (TFR) and the Swedish National Board for Industrial and Technical Development (NUTEK).

[1] P. A. Mitkas, L. J. Irakliotis, F. R. Beyette, Jr., S. A. Feld, and C. W. Wilmsen, Appl. Opt. **33**, 1345 (1994).
[2] N. Chand, P. A. Houston, and P. N. Robson, IEEE Trans. Electron Devices **32**, 622 (1985).
[3] O. Sjölund, M. Ghisoni, and A. Larsson, Electron. Lett. **31**, 917 (1995).
[4] H. T. Lin, D. H. Rich, O. Sjölund, M. Ghisoni, and A. Larsson, J. Appl. Phys. **79**, 8015 (1996).
[5] D. Bimberg, H. Münzel, A. Stechenborn, and J. Christen, Phys. Rev. B **31**, 7788 (1985).
[6] T. E. Everhart and P. H. Hoff, J. Appl. Phys. **42**, 5837 (1971).